Environmental Research 232 (2023) 116343

Contents lists available at ScienceDirect

Environmental Research

journal homepage: www.elsevier.com/locate/envres

Continuous atmospheric in-situ measurements of the CH_4/CO ratio at the Mt. Cimone station (Italy, 2165 m a.s.l.) and their possible use for estimating regional CH_4 emissions

C. Fratticioli [a], P. Trisolino [a], M. Maione [b], F. Calzolari [a], C. Calidonna [c], D. Biron [d], S. Amendola [d], M. Steinbacher [e], P. Cristofanelli [a,*]

[a] CNR-ISAC, Via Gobetti 101, 40129, Bologna, Italy
[b] University of Urbino - Faculty of Science and Technologies, Piazza Rinascimento 6, Urbino, 61029, Italy
[c] CNR-ISAC, Zona Industriale-Comparto 15-presso Fondazione Mediterranea Terina, I-88046, Lamezia Terme, CZ, Italy
[d] Aeronautica Militare, CAMM - Monte Cimone, Via delle Ville, 40 - 41029 Sestola, MO, Italy
[e] Empa, Ueberlandstrasse 129, 8600, Switzerland

ARTICLE INFO

Handling Editor: Robert Letcher

Keywords:
Methane
Carbon monoxide
Emissions
Italy
Inter-species correlation
ICOS

ABSTRACT

Methane (CH_4) is an important climate forcer, contributing about 17% of the total radiative forcing by long living greenhouse gases. The Po basin is one of the most polluted and densely populated areas in Europe representing an important source region for CH_4.

The aim of this work was to test an inter-species correlation approach to derive estimates of anthropogenic CH_4 emissions for the period 2015–2019 from the Po basin by combining CO bottom-up inventory data and continuous CH_4 and CO observations from a mountain site in the northern Italy. The tested methodology suggested lower emissions in respect to EDGAR (−17%) and the Italian National Inventory (−40%) for the Po basin. However, despite the two bottom-up inventories, the emissions derived from the atmospheric observations reported an increasing tendency from 2015 to 2019 for the CH_4 emissions. A sensitivity study revealed that using different subsets of the atmospheric observations implied a difference of 26% in the CH_4 emission estimates. The highest agreement with two bottom-up CH_4 inventories (EDGAR and the Italian national inventory) were obtained when atmospheric data were strictly selected for periods representative of air mass transport from the Po basin.

Our study identified various challenges when using this methodology as a benchmark to verify bottom-up CH_4 inventories. Issues could be attributed to the annual aggregation of the proxies used to derive the emission amounts, to the CO bottom-up inventory used as input information and to the relatively high sensitivity of the results to the different subsets of the atmospheric observations. However, the use of different bottom-up inventories as input data for CO emissions can potentially provide information that should be carefully considered for the purpose of integrating CH_4 bottom-up inventories.

1. Introduction

Methane (CH_4) is the second most important anthropogenic GHG, representing about 17% of the total radiative forcing by long living greenhouse gases. The global mean CH_4 mole fraction is constantly increasing over time, reaching 1908 ± 2 ppb in 2021, that is about 262% higher than the pre-industrial values, and showing an average yearly growth rate of about 9 ppb/year in the last decade (World Meteorological Organization, 2022). CH_4 is also a precursor of ozone (O_3) in the troposphere: reducing global CH_4 emissions will lead to reductions of the background O_3 with co-benefits for climate change, ecosystem integrity, crop yields and human health (Szopa et al., 2021). These are the reasons why on 17 September 2021, the European Union and the United States of America announced the Global Methane Pledge (GMP). Participants joining the Pledge agreed to take voluntary actions to contribute to the global goal of reducing CH_4 emissions by at least 30% by 2030 compared to 2020 levels (Caputo et al., 2022).

Total emissions of greenhouse gases (GHGs) by anthropogenic

* Corresponding author.
E-mail address: p.cristofanelli@isac.cnr.it (P. Cristofanelli).

https://doi.org/10.1016/j.envres.2023.116343
Received 28 March 2023; Received in revised form 21 May 2023; Accepted 5 June 2023
Available online 14 June 2023

activities are periodically estimated by national governments, international agencies and research institutes with the aim of monitoring emissions in the framework of national and international regulatory treaties. These estimates are generally provided by means of both "bottom-up" and "top-down" methods (Deng et al., 2022). While the former are based on the combination of socio-economic and geographical information (e.g. population density, land use, fuel consumption), the latter also rely on the use of atmospheric observations. In order to estimate total emissions of a given species, top-down methods use either the combination of atmospheric transport models with observed mole fractions (i.e. atmospheric inversion modelling) or the so-called "inter-species correlation", which is based on the analysis of the co-variability of a "reference" species to obtain information about the emissions of another pollutant or climate-altering compound (Flerlage et al., 2021). Being the emission estimates affected by different uncertainty contributions, these two approaches (i.e. "bottom-up" and "top-down") can be jointly used to provide more comprehensive estimation of uncertainties, to point out possible issues in the process of emission calculation and, finally, to provide more robust emission data (Cheewaphongphan et al., 2019; Nisbet and Weiss, 2010).

World-wide long-term CH_4 measurements have been coordinated since 1989 by the Global Atmospheric Watch program of the World Meteorological Organization (GAW/WMO) by taking advantage of measurements performed at global and regional stations. Moreover, recent efforts from the European Union led to the implementation of the Integrated Carbon Observation System (ICOS) Research Infrastructure (Heiskanen et al., 2022; http://www.icos-ri.eu) which provides, among several products, standardized and quality checked CH_4 data from a network of 37 atmospheric sites (ICOS RI et al., 2022).

At global scale, ~40% of atmospheric CH_4 is related to natural source emissions (e.g. wetlands, termites, seeps), while ~60% is attributed to anthropogenic sources (e.g. ruminants, rice agriculture, fossil fuel exploitation and distribution, waste management and combustion of biomass). In the atmosphere, the main sink for CH_4 (about 90% of the total sink) is the removal by hydroxyl radical (OH). By using top-down methodologies, CH_4 global emissions were estimated to be in the range 524–560 Tg CH_4 yr^{-1} for the period 2008–2017, while bottom-up approaches provide higher estimates of about 737 Tg CH_4 yr^{-1}, thus showing important inconsistencies in the two approaches (Saunois et al., 2020). Noteworthy, a recent work showed a fair consistency in CH_4 emission estimates by bottom-up and top-down approaches in the European region (Bergamaschi et al., 2022).The inconsistent results from different studies aiming at the estimation of CH_4 emissions and the important role of this species in the global radiative budget, highlights the need for further investigations. Moreover, level of agreement between bottom-up and top-down estimates can significantly change when down-scaling to regional and local scales.

Top-down approaches that analysed the inter-species correlation by using atmospheric observations (in-situ, remote-sensing, aircraft-based) were carried out in the last years to integrate bottom-up inventories and quantify GHG emissions from given regions (Anderson et al., 2021; Plant et al., 2022; Ren et al., 2018; Silva et al., 2013; Worthy et al., 2009).

While studying the source categories that affected CH_4 emissions from the Los Angeles basin (US), an interspecies correlation approach was used by Kuwayama et al. (2019), hereinafter KU2019. In this study, the authors used as input data a combination of in-situ atmospheric measurement of the CH_4/CO ratio at a station representative for air masses affected by emissions occurring over the source region, with CO emission data obtained from bottom-up inventories for the same source region.

This approach is rather simple (especially in terms of computational efforts) if compared to the more complex inversion methods, where the integration of atmospheric transport modelling, statistical Bayesian methods and a-priori bottom-up emission fields are required (Bergamaschi et al., 2018). In particular, KU2019 took advantage of the CH_4/CO ratio measured at the mountain site of Mt. Wilson, which is located at 1742 m a.s.l., overlooking Los Angeles city. This suggested that a similar method could be applied to other regions presenting relatively high emission rates, when compared to the surrounding regions, and where CH_4 and CO observations are available from a receptor site impacted by the emissions from the tagged source region. This site must be also far away enough to guarantee that the air masses emitted from the underlying source region are well mixed when reaching the measurement site, so that the atmospheric observations can be considered as representative of a sufficiently wide area. Nevertheless, before using a similar approach to other specific source regions, it is necessary to validate it and to assess different contributions to the overall uncertainty.

The Po basin is one of the most polluted and densely populated areas in Europe (Crippa et al., 2016), and it is strongly industrialised. The diversity of land use in the Po basin makes this region a contributor to GHGs emissions from different sources. Medium and large cities, as well as industrialised areas, contribute significantly to emissions from industrial processes, combustion, waste management and natural gas distribution. Large rural areas and intensive farming activity lead to important emissions related to agriculture and livestock sectors (Meijidea et al., 2017; Pezzagno et al., 2020).

The important contribution of the Po basin to the Italian national emission budget makes routine and accurate monitoring of natural and anthropogenic GHG emissions from this region to be pivotal. Up to now, no specific efforts have been pursued to use atmospheric observations to specifically quantify CH_4 emissions from this source region. Some information can be found in the recent inverse modelling exercise by Bergamaschi et al. (2022). In this work, three bottom-up inventories (i.e. EDGAR v6.0, TNO-VERIFY v3.0, GCP-CH_4) used for the prior estimates of CH_4 , identified the Po basin as a high emission area, with fluxes ranging from 15 to 50 mg CH_4 m^{-2} day^{-1} over different parts of the basin.

Here, we applied the interspecies correlation approach (KU2019) to the dataset of continuous CH_4 and CO observations at Mt. Cimone, the highest mountain of the Italian northern Apennines. Our goals were to determine the CH_4 emissions from the Po basin and to consider the source of uncertainties related to the different steps of this methodology and, finally, discuss the applicability of this methodology for estimating the CH_4 emissions. Moreover, a critical comparison of our results with the emission data provided by two "bottom-up" inventories is also provided.

2. Methodology

2.1. Measurement site

Continuous ground-based in-situ CH_4 and CO observations were performed at the Mt. Cimone station (CMN, 44° 11′ 38″ N, 10° 42′ 5″ E, 2165 m a.s.l.; Fig. 1) from January 2015 to December 2019.

During the daytime in the warmest months and during favourable meteorological conditions during the rest of the year, CMN is affected by the transport of air masses from the underlying Po basin which extends from North-West to the East of the measurement site (Cristofanelli et al., 2020). The "O. Vittori" atmospheric observatory is located about 50 m below the top of the mountain. It is a WMO/GAW global station and it has been labelled as an ICOS class-2 atmospheric site since May 2018. It is managed by the Institute for Atmospheric and Climate Sciences of the National Research Council of Italy (CNR-ISAC) in cooperation with the Italian Air Force (CAMM - Monte Cimone). The dominant circulation at the site is from the NE and SW sectors (Fig. 2).

In order to evaluate the representativeness of CMN observations for the Po basin emissions, the surface influence of the emissions occurring over northern Italy was calculated for different seasons for both CO and CH_4 by combining the footprints provided by the Stochastic Time Inverted Lagrangian Transport (STILT) model (Lin et al., 2003) with the EDGAR emission inventories for the two species (EDGARv6.0 for CH_4 ,

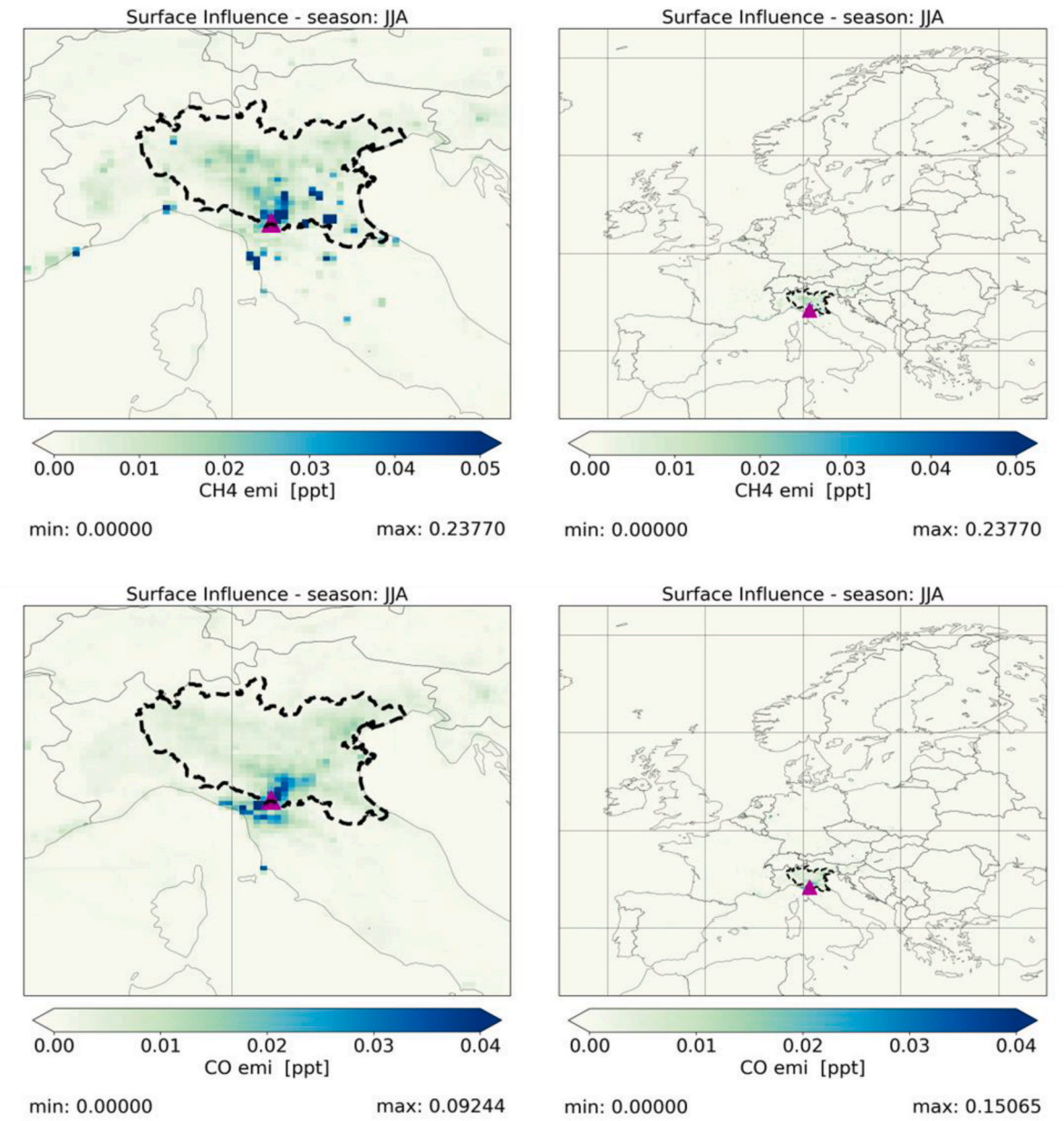

Fig. 1. Averaged surface influence for CH_4 (upper) and CO (bottom) during the studied period (2015–2019) for the June–August season (JJA). On the right, for comparison, the surface influence extended to the wider European domain isreported. The target emission region used in this study is included inside the dashed boundary. In order to compute the surface influence, STILT footprints were obtained from the icoscp.stilt python module (D'Onofrio and ICOS Carbon Portal, 2021) run on the icos-cp jupyter hub (https://exploredata.icos-cp.eu/), while the emission data were obtained from the EDGAR v6.0 and v6.1 inventories for CH_4 and CO respectively. Each pixel corresponds to a 0.1° × 0.1° grid point in the EDGAR inventory and STILT outputs. The pink triangle shows the CMN location.

EDGARv6.1 for CO, further details and references are reported in Section 2.4). The obtained results are reported in Fig. 1 for the June–August season (JJA), while the surface influence for the other seasons is shown in the supplementary material. Then, a "target" emission region was defined (dashed boundaries in Fig. 1) as the spatial region that maximised the relative contribution of the surface influence of emissions in respect to the whole European domain and that exhibited a fairly homogeneous emission pattern (more details about the definition of the target emission region are reported in the Supplementary Material). Please note that the spatial boundaries of the administrative districts in the Po basin were used to define the target region. We evaluated the seasonal percentage contribution of the total surface influence inside the selected target emission region with respect to the wider European domain (Fig. 1, right). This percentage ranged between 12.2%-20.1% and 11.6%–21.5% for CO and CH_4 respectively, with higher values obtained during JJA. The higher surface influence of the selected target emission region in the summer period is likely to be related to the higher planetary boundary layer (PBL) height during the warmer months that, together with the development of mesoscale circulation, favor the transport of air masses from the Po basin to CMN (Cristofanelli et al., 2020).

2.2. CH_4 and CO measurements at CMN

Observations from January 2015 through December 2019 were used in this study to keep an homogeneous observation set-up for CH_4. Since January 2015 to April 2018, the CH_4 measurements carried out by CAMM - Italian Air Force and produced by measurements based on the Cavity Ring Down Spectroscopy technique (Picarro G2401) were considered. For the same years, CO observations were produced by CNR-

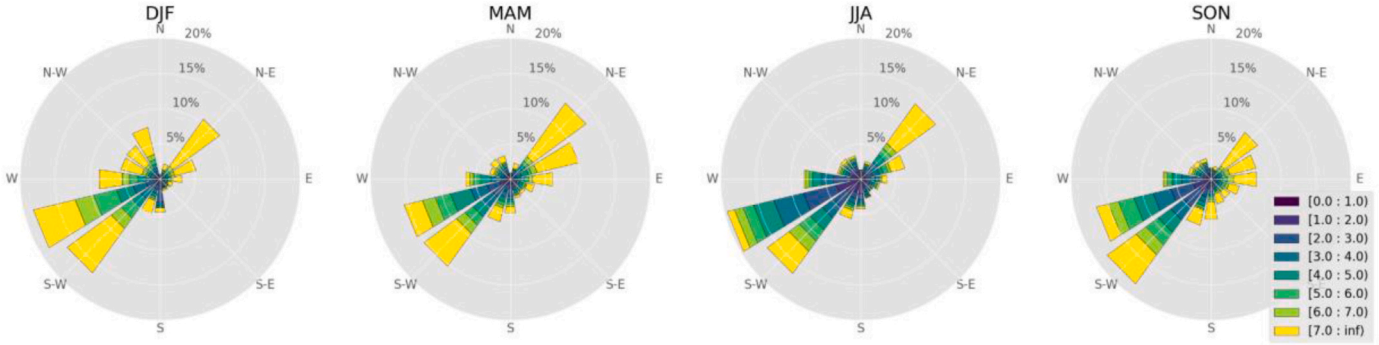

Fig. 2. Seasonal wind roses at CMN in 2015, 2016, 2018, 2019. The coloured scale report wind speed categories (m/s) as a function of the different sectors of wind origin.

ISAC using non-dispersive infrared (NDIR) absorption technique. The system was based on a Tei48C-TL analyser (Thermo Environmental), which uses gas filter correlation technology for determining CO ambient mole fraction (for more technical details see Cristofanelli et al. (2021a, b)). Both CH_4 and CO data were obtained from the World Data Centre for Greenhouse Gases (Cristofanelli et al., 2021a ; Italian Air Force Mountain Centre, 2022). CO mole fraction data for 2017 were not available due to the decommissioning of the NDIR instrument in this year.

Since May 2018, CO and CH_4 observations have been carried out in the framework of the ICOS research infrastructure. The CMN site was approved as an ICOS atmospheric class 2 site in November 2018 with measurements being available since May 2018. Within ICOS, atmospheric observations of CO and CH_4 are carried out in a standardised way for the measurement set-up, used materials, quality assurance strategy and data creation workflow (Hazan et al., 2016; Yver-Kwok et al., 2021). The dataset considered in this work is part of the ICOS level-2 data release (1-hourly time averaged data that underwent the final quality check, Cristofanelli and Trisolino, 2022a, b).

The monthly CO mole fraction (median values) at CMN ranged from an average monthly value of 170 ppb in February 2018 to 90 ppb in December 2016 (Fig. 3). Among the different years, a seasonal cycle typically occurred with the highest values in late winter/early spring and minima in summer/autumn (Cristofanelli et al., 2013). In respect to 2016–2019, higher CO values were observed at CMN during 2015. In particular, CO high values were observed during the warm months on 2015: the averaged CO mole fraction on June–September was +31 ppb higher than the following year. The inspection of the dataset provided by

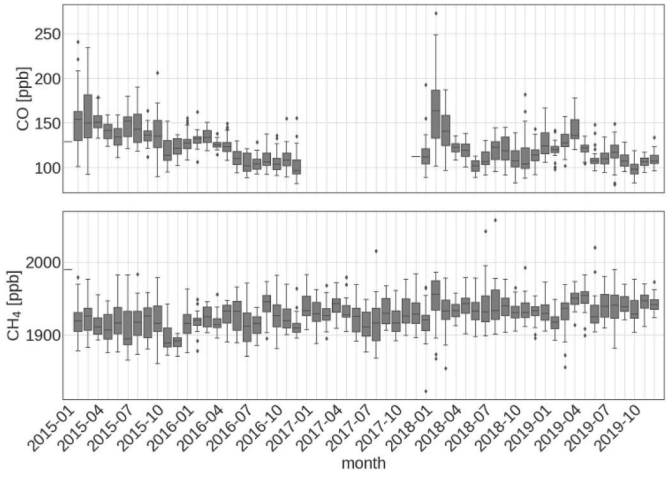

Fig. 3. Monthly boxplot of hourly averaged CO (upper) and CH_4 (bottom) observed d at CMN from January 2015 to December 2019. For each calendar month, the box-and-whiskers plot denote the 5th, 25th, 50th, 75th and 95th percentile of the hourly mean values while circles donate outlier data.

the World Data Center for Greenhouse Gases (https://gaw.kishou.go.jp/) revealed that CO increases (but lower than at CMN) were observed also at other measurement sites in Europe. As an instance, in respect to 2016, the period June–September 2015 reported +9 ppb at Jungfraujoch (46.54°N, 7.98°E, 3580 m a.s.l.; Switzerland; Seitz and Steinbacher, 2022), +12 ppb at Payerne (46.81°N, 6.94°E, 490 m a.s.l.; Swizterland; Seitz, 2022), +16 ppb at Mt. Zugspitze (47.42°N, 10.98°E, 2671 m a.s.l.; Germany; Couret, 2022) and +10 ppb at Mt. Sonnblick (47.05°N, 12.96°E, 3106 m a.s.l.; Austria; Spangl and Buxbaum, 2022). The inspection of the observations at these other European sites suggested that different processes occurring at local and larger spatial scales may have contributed to the observed CO values at CMN.

As expected, the time series of the CH_4 is characterised by an increasing trend from 2015 to 2019. It is difficult to find a clear seasonal cycle in the CH_4 observations, however the highest monthly 95th percentiles were usually observed during the summer months, possibly tracing the enhanced vertical transport of air masses from the Po basin.

2.3. Calculation of the Po basin CH_4 total emission

In-situ measurements of CH_4 and CO mole fractions were combined with CO emission data obtained from two bottom-up emission inventories. By supposing that the air masses that travelled from the target emission region to the observatory were well mixed and that anthropogenic-emitted CH_4 correlates with observed CO, CH_4 and CO in-situ measurements can be combined with CO emission data from bottom-up inventories by following KU2019:

$$M_{CH_4}[t] = S_{CH_4/CO}[t] \times M_{CO}[t] \times \frac{{M_{mol}}^{CH_4}}{{M_{mol}}^{CO}} \quad (1)$$

where $M_{CH4}[t]$ and $M_{CO}[t]$ are the total CH_4 and CO masses emitted from the target emission region during the t^{th} year, as obtained by emission inventories, $S_{CH4/CO}[t]$ is the yearly averaged slope obtained by orthogonal regression of the in-situ CH_4 and CO, M_{mol}^{CH4} and M_{mol}^{CO} are the molar masses of CH_4 and CO respectively. According with KU2019, the yearly averaged slope $S_{CH4/CO}$ is obtained by the observed CH_4 and CO values at CMN (see Section 2.5). Due to the proximity of the emission region to the measurement site, we assumed a low impact on the $S_{CH4/CO}$ ratio by the seasonal CO lifetime variation in the atmosphere related to the OH radical removal.

Equation (1) was then used to evaluate CH_4 emissions by using as input the M_{CO} value from two bottom-up inventories and the slope $S_{CH4/CO}$ obtained by the orthogonal regressions of the CMN observations.

The total uncertainty $\Delta M_{CH4}[t]$ was obtained from Equation (2) and it is equal to:

$$\Delta M_{CH_4}[t] = \left(\frac{\Delta S_{CH_4/CO}[t]}{S_{CH_4/CO}[t]} + \frac{\Delta M_{CO}[t]}{M_{CO}[t]}\right) M_{CH_4}[t] \quad (2)$$

where ΔM_{CO} [t] represented the error related with the CO emission from bottom-up inventories (Section 2.4), while $\Delta S_{CH4/CO}[t]$ represented the error related with the yearly slope $S_{CH4/CO}$ described in Section 2.5.

2.4. The EDGAR and ISPRA emission inventories

Two "bottom-up" inventories were considered in this study: (i) the Emissions Database for Global Atmospheric Research (EDGAR) (Crippa et al., 2021, 2022) that is released by the Joint Research Centre (JRC) of the European Commission and (ii) the Italian National inventory that is released by the Italian National Institute for Environmental Protection and Research, hereinafter "ISPRA" (Romano et al., 2022). The EDGARv6.0 inventory was used for getting bottom-up CH_4 emissions (Crippa et al., 2021), while EDGARv6.1 (Crippa et al., 2022) was used for CO emissions.

The EDGAR and ISPRA inventories differed in the spatial resolution and coverage: while EDGAR is a global inventory that reports worldwide anthropogenic emissions on a $0.1^\circ \times 0.1^\circ$ spatial grid, the inventory provided by ISPRA is available only for Italy and the emissions are aggregated over Italian administrative districts. For what concerns the ISPRA inventory, district-based emission data were obtained by the disaggregation of the national emission values (Istituto Superiore per la Protezione e la Ricerca Ambientale, 2022).

Being emission inventories based on the statistical elaboration of socio-economic and geographical information, the results are generally provided with time resolution ranging from one to a few years. In this study, we relied on the emission estimates with a time resolution of one year. However, while EDGAR provided emissions for each year in range 1970–2018, ISPRA provided data every 5 years during the period 1990–2015, plus the year 2019. EDGAR emission also provided temporal profiles to derive emissions with monthly resolution (Crippa et al., 2019). However, for keep the consistency between the two bottom-up databases, the yearly aggregation was considered also for EDGAR. For what concerns the ISPRA inventory, a linear interpolation was performed in order to obtain values for years 2016 and 2018. Since we wanted to focus to anthropogenic emissions and to harmonise the overall analysis, categories related to natural sources (waters, wetlands, fires, gas seeps, i.e. category 11 of ISPRA inventory) were not considered.

The accuracy of the estimated emissions is strongly related to the availability of socio-economic and geographical information at each grid point or for each state/region, leading in general to more precise estimates in developed countries. In order to fulfil the requirements of the international framework (e.g. the United Nations Framework Convention on Climate Change - UNFCCC) the quantification of the total uncertainty related to the emissions is required, at least for what concerns GHGs.

Total emissions in bottom-up inventories are obtained by the addition of total emissions from different source categories, which for the EDGAR and ISPRA inventories are defined by Eggleston et al. (2006). Each source category is used to group anthropic processes that have similar emission patterns (e.g. transportation, agriculture, waste management), with each source category that can be divided in subcategories (e.g. enteric fermentation, manure management and rice cultivation are subcategories for the agriculture category). For each source category and subcategory, specific Emission Factors (EFs) and Activity Data (AD) are defined. They represent, respectively, the emissions for unity of activity (e.g. mean CO emissions per km per car) and the activity of the respective source category (e.g. number of cars and travelled km per year). By combining EFs with AD, total emissions are obtained for each source category.

Being total emissions obtained by the product between EFs with AD and supposing uncorrelation of different source categories (Bergamaschi et al., 2015), their uncertainty is given by:

$$u = \sum_i \sqrt{(u_{EF})_i^2 + (u_{AD})_i^2} \quad (3)$$

where u_{EF} and u_{AD} are the uncertainties related to EFs and AD and i refers to the i^{th} source category. Both EDGAR and ISPRA inventories provided u_{EF} and u_{AD} for different source categories for the main GHGs (Romano et al., 2022; Solazzo et al., 2021), thus allowing the calculation of the total uncertainty for the CH_4 total emission.

For what concerns the ISPRA inventory, Equation (3) was used in order to estimate the uncertainty related to emissions from the seven key categories (i.e. the ensemble of source categories that contribute more than 90% to the total uncertainty) in Italy for CH_4 (4.D.1 domestic wastewater, 4.D.2 industrial wastewater, 4.C solid waste, 3.C.7 rice cultivation, 1.B.2 fugitive emissions, 3.A.1 enteric fermentation, 3.A.2 manure management). By adopting the values of u_{EF} and u_{AD} and the total national emissions of CH_4 in 2020 which are reported in Romano et al. (2022), we inferred a relative emission uncertainty of 17% for the whole Italy. By adopting the values of u_{EF} and u_{AD} reported in Solazzo et al. (2021), a relative emission uncertainty of 37% was obtained for EDGAR v6.0.

For the ISPRA dataset, we assumed that the national-scale CH_4 emission uncertainties are representative also for our regional domain. This choice can be questionable, considering that differences in the relative weight of specific category emissions exist moving from the national to the regional domain.

Up to now, the EDGAR and ISPRA uncertainties on EFs and AD were officially released only for GHGs, thus not allowing the uncertainty estimation for CO emissions. To overcome this problem, we considered the mean relative difference between the CO emissions obtained from the EDGAR and ISPRA inventories over the period 1990–2019 (1.37 Mt and 1.18 Mt, respectively) as a possible estimation of the uncertainty related to the CO emissions for the two inventories. The obtained relative uncertainty is equal to 14.9%. The same method applied to CH_4 emissions led to a relative uncertainty equal to 13.9%, that represents the 82% and the 38% of the uncertainties estimated explicitly by using u_{AD} and u_{EF} for the ISPRA and EDGAR inventories. By applying the scaling factors valid for CH_4 uncertainties, we obtained CO emission uncertainties of 18.9% for ISPRA and 39% for EDGAR.

2.5. Calculation of yearly average observed slope CH_4/CO

According with KU2019, the yearly averaged slope $S_{CH4/CO}$ is obtained by calculating orthogonal regressions over monthly aggregated hourly values of observed CH_4 and CO and by averaging the monthly slope values over the whole year. As suggested by KU2019, each monthly dataset was tested in order to retain only results from robust regressions. This test consisted in performing multiple regressions on different random subsets of the original dataset and by requiring that the results from the different subsets do not differ more than a given threshold. According to KU2019, we calculated the mean slopes of each single year by averaging the monthly $S_{CH4/CO}$ that passed the robustness test. The error associated to the slope (i.e. $\Delta S_{CH4/CO}$ in Equation (2)) was evaluated as the 95% confidence interval of the mean $S_{CH4/CO}$ value. Monthly regressions for 2019 on the original dataset are reported in Figure SM5 in the supplementary material as an example.

It should be considered that the target emission region considered by KU2019 for the Los Angeles basin was much more homogenous than the Po basin. In particular, the signal of emissions from the Po basin caught by CMN can be mixed with those from other national regions as well as from continental European regions upwind from the Po basin. Thus, it was necessary to subset the CMN observations to retain periods that are more representative of emissions from the Po basin. To this aim, different data selection criteria were considered and tested. A first data selection was made by only considering daytime observations in order to select the air masses that could have been transported to CMN through

convection and upslope/up-valley mountain thermal winds (see Cristofanelli et al., 2020). The selection over daytime was performed using the python sunset module (https://pypi.org/project/suntime/) to get sunrise and sunset times at CMN for each day: daytime measurements were defined as those measurements between 3 h after sunrise and 3 h before sunset.

A further selection was performed based on the wind direction (WD) in order to specifically select CMN observations representative of local circulation transporting air masses from the Po basin (WD in the range from 310° to 80°, hereinafter "WD: 310-80").

Moreover, the output of the Background Data Selection fit (BaDSfit) algorithm (Trisolino et al., 2021) was considered in order to select the observations that were carried out in non-background conditions (i.e. measurements influenced by regional fluxes, hereinafter "Non-bkg"). In order to eliminate possible outliers in the BaDSfit output, only non-background conditions that lasted at least three consecutive hours were retained in the analysis. A stricter criterion was also set by considering observation data that simultaneously satisfied the "WD: 310-80" and the "Non-bkg" conditions (hereinafter "Non-bkg + WD 310-80").

Finally, a further data selection based on the WD was considered to obtain a "control" case: we selected observations recorded under south-easterly local circulation (WD in range from 110° to 180°) to catch measurement conditions representative for the air-mass transport from a near region but different than the Po basin (i.e. Tuscany and Liguria Sea). The results from this last selection were compared with the others to provide hints about the actual added value of the atmospheric observations in estimating emissions from the Po basin.

A further point that should be considered is that the annual variability of the CMN monthly $S_{CH4/CO}$ values was larger than for the Los Angeles basin (Figure SM6 in the supplementary material). This is probably related to the different emission profiles characterising the Po basin region in respect to the Los Angeles basin (see related discussion in the supplementary material). By using yearly averaged $S_{CH4/CO}$ values instead of seasonal or monthly values can potentially introduce uncertainties in emission calculation when specific emission categories have strong seasonality (like the case of rice cultivation in the Po basin or livestock manure, see Meijidea et al. (2017) and Chen et al. (2018)). The potential impact to our estimate in considering seasonal $S_{CH4/CO}$ is discussed in Section 3.3.

3. Results and discussion

3.1. $S_{CH4/CO}$ values

For each single year included in the study period, the different values obtained for $S_{CH4/CO}$ as a function of the different subset of the original dataset were reported in Table 1. The mean value of the yearly slope varies between a minimum of 0.9 for 2015 when selecting observations recorded under "WD: 310-80", and a maximum of 1.6 for 2019 when selecting observations recorded under "Non-bkg".

In general, the calculated $S_{CH4/CO}$ had higher mean yearly values when the data were subset for non-background conditions and wind coming from the Po basin sector. An increasing tendency of the $S_{CH4/CO}$ values was generally observed over the considered years. Nevertheless, all the different $S_{CH4/CO}$ were consistent among each other when their errors are considered, thus the existence of temporal trends and significant differences among data subsets cannot be clearly stated.

Since CH_4 is affected by a global scale increasing trend, we also calculated the slope $S_{CH4/CO}$ after removing the global long-term trend (WMO, 2022). The long-term trend was diagnosed by using the CH_4 time series recorded at the high Alpine site Jungfraujoch (46.54° N, 7.98° E; 3580 m a.s.l.) from 2005 to 2021 (Steinbacher, 2022) by applying the "ccgcrv" method developed by Thoning et al. (1989). No significant changes with respect to the values reported in Table 1 were found when detrended CH_4 observations were considered. The same test was not performed for CO: even if CO is affected by significant year-to-year and seasonal variabilities at global scale, a clear trend cannot be observed over the period 2015–2019 (Japan Meteorological Agency and World Meteorological Organization, 2022).

3.2. CH_4 emissions based on bottom-up emissions

For the studied period, total CH_4 and CO emissions from the target region were obtained from both ISPRA and EDGAR inventories with their relative uncertainties (Fig. 4).

Generally, the two bottom-up datasets agreed (within the estimated uncertainties) in depicting declining emissions over the Po basin for CO and CH_4. Both EDGAR and ISPRA reported stronger declining CO emissions from 1990 to 2005. From 2010, they diagnosed a levelling-off of the CO decrease. The higher temporal resolution provided by EDGAR provides some information about the year-to-year variability of emissions. According to EDGAR, the emission peak occurred from 1993 to 1996 over the Po basin, a temporary levelling-off occurred from 2006 to 2008 and a renewed (but less intense) declining tendency occurred around 2010. In 2019, the total CO emissions from the Po basin were −72% and −70% than 1990, for ISPRA and EDGAR respectively. In general, the ISPRA inventories reported lower emissions than EDGAR, with absolute differences between the two inventories decreasing in recent years.

A different picture characterised the CH_4 emissions. Like for CO, both the bottom-up dataset agreed within their uncertainties. The ISPRA inventory reported higher CH_4 emissions than EDGAR (+8% from 2015 to 2019). In 2019, the total CH_4 emissions diagnosed by ISPRA and EDGAR were −22% and −24% than those reported for 1990. These values are largerthan the total National reduction of −13.4% reported by ISPRA from 1990 to 2020 (Caputo et al., 2022). Both the inventories suggested an almost monotonic decreasing tendency for CH_4 emissions with an average declining rate of 6 kt/year (equivalent to 0.8%/year). These numbers highlight the need for further efforts to meet the target on emissions set by the GMP (−30% by 2030 compared to 2020, equivalent to a decrease of −3%/year) at regional scale. Moreover, the averaged deviation (6%) between absolute EDGAR and ISPRA emission values represents a not-negligible fraction (20%) of the reduction goal set

Table 1
Yearly average slope $S_{CH4/CO}$ and related error for each year obtained from the original dataset (all data) and from different subsets of the original dataset. "daytime": only data between 3 h after sunrise and 3 h before sunset time. "WD: 310-80": only data with wind direction in range 310°–80°. "WD: 110–180": only data with wind direction in range 110–180°. "Non-bkg": only data corresponding to non-background conditions according to the BaDSfit algorithm. The slopes and their errors are equal to the mean value of the months that passed the robustness test and to the 95% confidence interval of the mean value respectively. In the "Mean" column are reported the mean value and the relative error of the respective year after averaging over the different subsets of the original dataset. Within brackets, the percentage of the data selected for the different subsets in respect to the whole dataset is reported.

	all data	daytime	WD:310-80	WD:110-180	Non-bkg	Non-bkg + WD:310-80	Mean
2015	1.0 ± 0.2	1.0 ± 0.2 (28%)	0.9 ± 0.2 (27%)	1.3 ± 0.5 (9.2%)	1.0 ± 0.3 (7.9%)	1.2 ± 0.4 (3.9%)	1.1 ± 0.3
2016	1.2 ± 0.5	1.2 ± 0.2 (27%)	1.2 ± 0.3 (20%)	1.2 ± 0.2 (6.3%)	1.2 ± 0.4 (8.6%)	1.6 ± 0.5 (3.3%)	1.3 ± 0.3
2018	1.1 ± 0.2	1.3 ± 0.3 (26%)	1.4 ± 0.3 (38%)	1.3 ± 0.3 (9.4%)	1.3 ± 0.3 (5.0%)	1.5 ± 0.4 (3.9%)	1.3 ± 0.3
2019	1.4 ± 0.2	1.4 ± 0.3 (26%)	1.4 ± 0.3 (28%)	1.3 ± 0.1 (9.6%)	1.6 ± 0.2 (9.5%)	1.5 ± 0.3 (5.5%)	1.4 ± 0.2

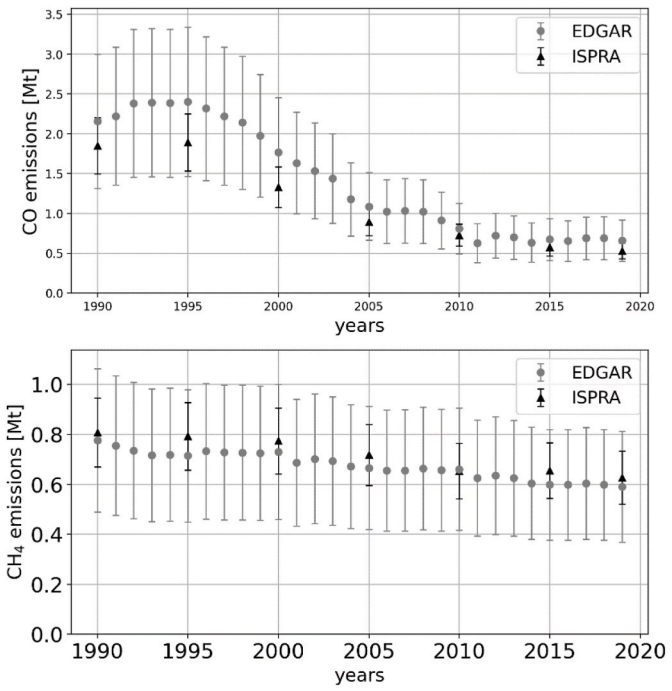

Fig. 4. CO (top) and CH_4 (bottom) total emissions from the target region obtained from ISPRA (excluding natural sources) and EDGAR inventories. Error bars for EDGAR and ISPRA were estimated following the procedure described in Section 2.4.

within the GMP in 2030. A better understanding of these deviations can help local policymakers in defining the correct road-map to achieve the emission reduction goals.

3.3. CH_4 emissions based on CMN observations

To provide a semi-independent assessment of the total CH_4 emissions from the Po basin, the method presented in Section 2.3 was applied to the CMN observations for each single calendar year (2015, 2016, 2018, 2019). As stated before, the year 2017 was excluded because of the absence of a continuous time series for CO at CMN, while years 2020 and 2021 were excluded due to the absence of data for the ISPRA inventory. Moreover, the COVID-19 pandemic and its related restrictions could lead to significant variations of total emissions in these years (Le Quéré et al., 2020) which cannot be assessed by extrapolating data from previous years.

Equation (1) was applied twice by using the total yearly CO emissions obtained from the EDGAR and ISPRA inventories as $M_{CO}[t]$ values and the yearly slope values reported in Table 1 as $S_{CH4/CO}[t]$ values.

In Fig. 5 is reported the total yearly Po basin CH_4 emissions for EDGAR (plate A) and ISPRA (Plate B) inventories together with calculated M_{CH4}^{ISPRA} and M_{CH4}^{EDGAR}. To assess the sensitivity of M_{CH4} calculation as a function of the different subsets of the CMN observations, we reported M_{CH4}^{ISPRA} and M_{CH4}^{EDGAR} as obtained for *(i)* the whole CMN dataset, (*ii*) daytime, (*iii*) WD from the Po basin sector (WD from 310° to 80°), (*iv*) non-background observations, (*v*) non-background observations and WD from the Po basin and (*vi*) from the control subset (WD from 110° to 180°). The M_{CH4}^{ISPRA} and M_{CH4}^{EDGAR} uncertainties were obtained by combining the uncertainties related with the different terms of Equation (1): thus they were larger than those obtained for the bottom-up inventories.

For the single years, the differences between the M_{CH4}^{EDGAR} values obtained by the various subsets of the CMN observations varied from 18% (2019) to 26% (2015). When compared with EDGAR CH_4 emissions, our M_{CH4}^{EDGAR} estimates diagnosed lower values for the different years and for

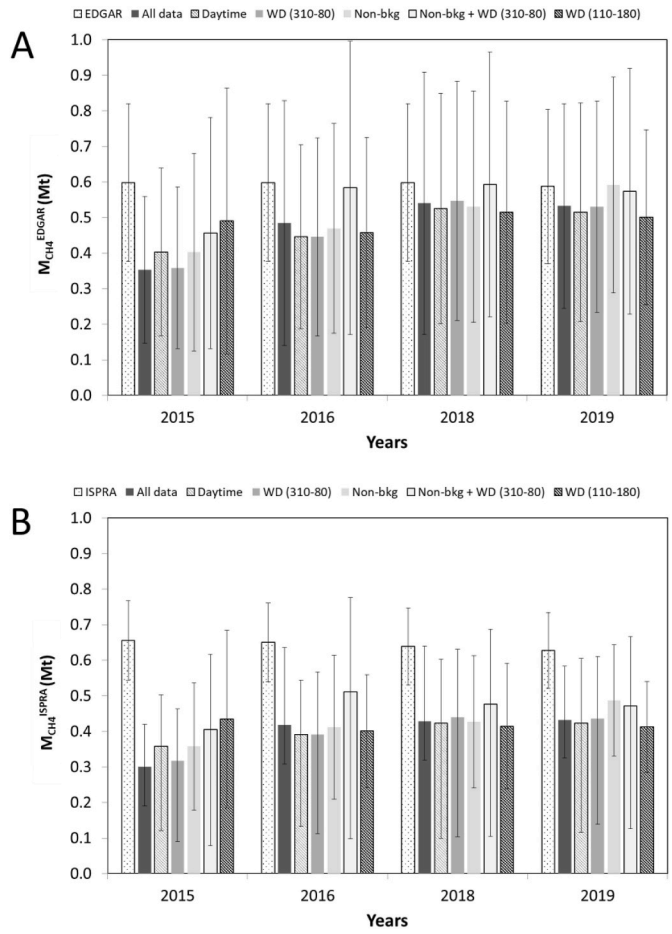

Fig. 5. CH_4 emissions obtained from bottom-up inventories (A: EDGAR, B: ISPRA) and estimated using Equation (1).

the different data subsets (from −30% in 2015, to −7% in 2019). Despite constant CH_4 emissions reported by the EDGAR inventory, our estimates were mostly characterised by an increasing tendency from 2015 to 2019: the observed increase ranged from +28% to +48%, depending on the different subsets (*i-vi*) of CMN data. The CH_4 emission estimated based on the "Non-bkg + WD (310-80)" CMN data selection were equal than those provided by EDGAR for years 2016, 2018 and 2019.

The yearly M_{CH4}^{ISPRA} values were also lower than the original data provided by the ISPRA inventory. When compared with ISPRA CH_4 emissions, our M_{CH4}^{ISPRA} estimates diagnosed lower values for the different years and for the different data subsets (from −48% in 2015, to −34% in 2019). Similarly to what was observed for the EDGAR case, the CH_4 emissions derived by using CMN observations were mostly characterised by an increasing tendency over the period 2015–2019. Nevertheless, also in 2019, the estimated M_{CH4}^{ISPRA} were lower than the bottom-up inventory (−34%). On average, M_{CH4}^{EDGAR} and M_{CH4}^{ISPRA} agreed within 18% over 2015–2019. An average difference of +15% was instead calculated between the two original ISPRA and EDGAR inventories. The application of the methodology by KU2019 led to a stronger decrease of the original ISPRA CH_4 emission data due to the lower CO emissions reported by ISPRA (Fig. 4, top). It is interesting to note that the differences with EDGAR and ISPRA inventories were minimised when the subset of CMN observations in non-background conditions and WD from the Po basin ("Non-bkg + WD (310-80)", see Fig. 5) were considered. The very strict selection criteria adopted for the "Non-bkg + WD (310-80)", lead to the selection of a relatively low number of observations (Table 1): this stresses the importance of performing continuous atmospheric observations with high time resolution to obtain a sufficient quantity of representative data.

For what concern the results obtained for the "control" subset of the CMN data (i.e. WD from 110° to 180°), we obtained M_{CH4}^{EDGAR} and M_{CH4}^{ISPRA} values that were in the range of the other data subsets. Only in respect to the most strict selection criterion "Non-bkg + WD (310-80)", the control case reported lower CH_4 emissions (for 3 out of 4 years). One explanation could be related to the fact that specific high emission areas of CO and CH_4 were present along the western coast-line of northern Italy (Fig. 1), leading to $S_{CH4/CO}$ values similar to those observed for the Po basin (Table 1). This would suggest that extreme caution must be used in interpreting the results from studies based on the interspecies correlation methodology, especially if observation data are not subset for measurement conditions representative of the air-mass transport from the source region.

As described in Section 2.5, according with the approach by KU2019, we used the yearly mean $S_{CH4/CO}$ value for scaling the regional CO inventories and obtaining CH_4 emission estimates for the Po basin. Since the monthly $S_{CH4/CO}$ values were characterised by an evident seasonal variability at CMN (see Figure SM2 in the supplementary material), we assessed the impact of using seasonal $S_{CH4/CO}$ values instead of the mean yearly $S_{CH4/CO}$ to the CH_4 emission obtained by Equation (1). To this aim, Equation (1) was applied to the CO emission by EDGAR and ISPRA data but using $S_{CH4/CO}$ calculated for October–March and for April–September. In general, by adopting the $S_{CH4/CO}$ obtained for the cold months lead to lower CH_4 emissions (ranging from −35% to −3% as a function of the different year and data subset). On the other side, by adopting the $S_{CH4/CO}$ calculated for the warm months lead to higher emissions (from 0% to 44%). As an example, for the data subset "Non-bkg + WD (310-80)", when the $S_{CH4/CO}$ obtained for cold months were considered, the calculated CH_4 emissions decreased by −33% on 2015, -28% on 2016, -32% on 2018 and -9% on 2019. On the other hand, when the $S_{CH4/CO}$ obtained for warm months were considered, the emissions increased by 20% on 2015, 0% on 2016, 21% on 2018 and 15% on 2019. This means that, despite the two emission bottom-up inventories, increasing trends of CH_4 emissions were still observed from 2016 to 2019 even if seasonal $S_{CH4/CO}$ were considered. It is interesting to note that when the $S_{CH4/CO}$ calculated for April–September were used, our calculated CH_4 emission were higher than EDGAR and ISPRA on 2018 and 2019. The higher CH_4 emissions obtained by considering the $S_{CH4/CO}$ calculated during the warm months would suggest that adopting yearly-averaged proxies for the emission calculation would potentially underestimate the contributions from source categories characterised by a significant seasonal behaviour (e.g. rice paddies and livestock manure).

A further point of concern was related to the possible impact of the long-range air mass transport to the variability of the ratio CH_4/CO observed at CMN and, thus, on the representativeness of CMN observations for the regional emissions. In fact, the application of the KU2019 method at CMN relied on the hypothesis that the CH_4/CO variability at the measurement site was representative of the emissions from the underlying target emission region. As shown in Section 2.1, for CMN, the surface influence of the target emission region considered in our study ranged from 11% to 22% of the total surface influence of the European domain. This would suggest that emission signals related with long-range transport could play a significant impact on the observed CH_4/CO variability. The subset of the CMN observations obtained by imposing conditions on the wind regime and on BaDSfit results could help in increasing the representativeness of CMN observations in respect to the emissions from the Po basin. Nevertheless a remaining contribution related to trans-boundary air mass transport cannot be ruled out. To better elucidate this point, we performed a test in which the CH_4/CO ratio was calculated by using deviations of hourly mean values in respect to the baseline calculated according to BaDSfit (Apadula et al., 2019; Thoning et al., 1989; Trisolino et al., 2021) (a detailed description of the baseline calculation is reported in the supplementary material). Indeed, the deviations of the measurements in respect to an atmospheric baseline would further help in retaining the signal of regional sources or sinks (Brantley et al., 2014; Drewnick et al., 2012; El Yazidi et al., 2018; Giostra et al., 2011). The test was carried out for the "Non-bkg + WD (310-80)" CMN data selection: no significant differences were found in respect to using absolute CH_4 and CO values. This would support that the obtained results were not significantly hindered by the contribution related to the long-range air mass transport.

Finally, it should be pointed out that natural emissions were not reported by EDGAR and we did not consider natural emissions in the ISPRA inventory (which represented 17% of the total anthropogenic emission over the period 2015–2019). Due to the diffuse presence of gas seeps and wetlands, the natural emissions represent an important contribution to the overall CH_4 budget over the Po Basin. In our approach, we considered CO as a "reference" species to derive the anthropogenic CH_4 emission and as a "surrogate" for tracing the transport of well-mixed air massed affected by emissions from the Po basin. These assumptions could represent a simplification because naturally-emitted CH_4 is mixed with anthropogenic-emitted CH_4 within the air masses observed at CMN. However, we assumed that naturally-emitted CH_4 emissions have had a weaker correlation to CO with respect to anthropogenic-emitted CH_4. In this case, the presence of naturally-emitted CH_4 would affect only marginally the observed $S_{CH4/CO}$ values and, thus, the emission values obtained by the KU2019 method. On the other side, assuming that the calculated estimates were also representative for the contribution from natural emissions would imply a substantial overestimation of the bottom-up inventories in respect to the KU2019 method.

4. Conclusions

In this work, we tested the application of an interspecies correlation top-down methodology to derive yearly CH_4 emissions from the Po basin region in northern Italy.

The comparison with the CH_4 emission data from the two bottom-up inventories, revealed lower emissions when the tested methodology is used (−40% in respect to ISPRA and −17% in respect to EDGAR over years 2015–2019, on average). Interestingly, despite the two bottom-up inventories, the CH_4 emissions derived from the CMN atmospheric observations mostly revealed an increasing tendency from 2015 to 2019.

The obtained results were sensitive to the data selection performed on the measured atmospheric data with the range of the emission estimates varying by 18%–26%. When using similar approaches, a "control" case designed to select air masses which did not have obvious origin from the target emission region should be considered to evaluate the effectiveness of the considered atmospheric observations in estimating the targeted emissions. For the Po basin case, we suggest to use the CMN observation periods characterised by non-background conditions and local wind from the NE sector which also lead to an higher consistency with bottom-up inventories.

Further uncertainties can arise from the annual aggregation of the proxy (i.e. the slope $S_{CH4/CO}$) used to derive the CH_4 emissions because specific emission categories can have a strong seasonality behaviour (like rice cultivation emissions or livestock manures in the Po basin).

The results provided by the applied methodology were also sensitive to the CO emissions provided by the bottom-up inventories which are scaled by the slope of the observed CH_4/CO correlation. Accurate CO emission data are of paramount importance for a correct application of this methodology. Since uncertainties of bottom-up CO inventories were around 20% (or even higher, see Crippa et al., 2018), important questions should be raised about the effectiveness of using CO emission data as reference for obtaining CH_4 emissions. The alternative or combined use of other atmospheric tracers sensitive to CH_4 emission sources (like ^{222}Rn, CO_2, specific volatile organic compounds, stable CH_4 isotopes) can represent further constraints to provide more robust results.

To summarise, it looked challenging to use this methodology as a "solid" benchmark to evaluate the quality of bottom-up CH_4 inventories, especially when a representative study of the atmospheric observations

and an uncertainty quantification of CO bottom-up inventories are not available. However, the use of different CO bottom-up inventories to obtain an "ensemble" of results can potentially provide information to highlight possible differences with CH_4 bottom-up inventories (see e.g. the increasing CH_4 emission tendency observed for the Po basin) and to start a process of attribution involving the compilers of bottom-up inventories.

Credit author statement

Cosimo Fratticioli: Software, Methodology, Formal analysis, Investigation, Writing – Original Draft, Visualization**. Pamela Trisolino:** Data curation, Writing – Review and Editing. **Michela Maione:** Conceptualization**,** Data curation, Writing – Review and Editing. **Francescopiero Calzolari:** Data curation, Writing – Review and Editing. **Claudia Calidonna:** Project administration, Funding acquisition**. Daniele Biron:** Data curation, Writing – Review and Editing. **Stefano Amendola:** Data curation, Writing – Review and Editing. **Martin Steinbacher:** Data curation, Validation, Writing – Review and Editing. **Paolo Cristofanelli:** Conceptualization, Methodology, Formal analysis, Investigation, Resources, Data Curation, Writing – Original Draft, Visualization, Project administration, Funding acquisition**.**

Declaration of competing interest

The authors declare that they have no known competing financial interests or personal relationships that could have appeared to influence the work reported in this paper.

Data availability

Reference to the data used, including doi when available, are provided in the manuscript

Acknowledgments

CNR-ISAC acknowledges the ICOS Atmospheric Thematic Center (ATC) for the support in the production of the CH_4 and CO time series at the ICOS site IT-CMN and the Italian Air Force CAMM-Mt. Cimone for their support in the operation of the ICOS site. ICOS activities at CMN were supported by Joint Research Unit "ICOS Italia", funded by Ministry of University and Researches, throughout CNR-DSSTTA. Cosimo Fratticioli and Pamela Trisolino grants are funded by Ministry of University and Research trough "Progetto nazionale Rafforzamento del Capitale Umano CIR01_00019 – PRO–ICOS–MED "Potenziamento della rete di osservazione ICOS-Italia nel Mediterraneo – Rafforzamento del Capitale Umano".

Appendix A. Supplementary data

Supplementary data to this article can be found online at https://doi.org/10.1016/j.envres.2023.116343.

References

Anderson, D.C., Lindsay, A., DeCarlo, P.F., Wood, E.C., 2021. Urban emissions of nitrogen oxides, carbon monoxide, and methane determined from ground-based measurements in philadelphia. Environ. Sci. Technol. 55, 4532–4541. https://doi.org/10.1021/acs.est.1c00294.

Apadula, F, Cassardo, C, Ferrarese, S, Heltai, D, Lanza, A, 2019. Thirty Years of Atmospheric CO_2 Observations at the Plateau Rosa Station, Italy. Atmosphere 10 (7), 418. https://doi.org/10.3390/atmos10070418.

Bergamaschi, P., Corazza, M., Karstens, U., Athanassiadou, M., Thompson, R.L., Pison, I., Manning, A.J., Bousquet, P., Segers, A., Vermeulen, A.T., Janssens-Maenhout, G., Schmidt, M., Ramonet, M., Meinhardt, F., Aalto, T., Haszpra, L., Moncrieff, J., Popa, M.E., Lowry, D., Steinbacher, M., Jordan, A., O'Doherty, S., Piacentino, S., Dlugokencky, E., 2015. Top-down estimates of European CH_4 and N_2O emissions based on four different inverse models. Atmos. Chem. Phys. 15, 715–736. https://doi.org/10.5194/acp-15-715-2015.

Bergamaschi, P., Danila, A.M., Weiss, R., Ciais, P., Thompson, R.L., Brunner, D., Levin, I., Meijer, Y., Chevallier, F., Janssens-Maenhout, G., Bovensmann, H., Crisp, D., Basu, S., Dlugokencky, E., Engelen, R., Gerbig, C., Günther, D., Hammer, S., Henne, S., Houweling, S., Karstens, U., Kort, E., Maione, M., Manning, A., Miller, J., Montzka, S., Pandey, S., Peters, W., Peylin, P., Pinty, B., Ramonet, M., Reimann, S., Röckmann, T., Schmidt, M., Strogies, M., Sussams, J., Tarasova, O., Van, A.J., Vermeulen, A., Vogel, F., 2018. Atmospheric Monitoring and Inverse Modelling for Verification of Greenhouse Gas Inventories. JRC Publ. Repos. https://doi.org/10.2760/759928.

Bergamaschi, P., Segers, A., Brunner, D., Haussaire, J.-M., Henne, S., Ramonet, M., Arnold, T., Biermann, T., Chen, H., Conil, S., Delmotte, M., Forster, G., Frumau, A., Kubistin, D., Lan, X., Leuenberger, M., Lindauer, M., Lopez, M., Manca, G., Müller-Williams, J., O'Doherty, S., Scheeren, B., Steinbacher, M., Trisolino, P., Vítková, G., Yver Kwok, C., 2022. High-resolution inverse modelling of European CH_4 emissions using novel FLEXPART-COSMO TM5 4DVAR inverse modelling system. Atmos. Chem. Phys. Discuss. 1–37. https://doi.org/10.5194/acp-2022-118.

Brantley, H.L., Hagler, G.S.W., Kimbrough, E.S., Williams, R.W., Mukerjee, S., Neas, L. M., 2014. Mobile air monitoring data-processing strategies and effects on spatial air pollution trends. Atmos. Meas. Tech. 7, 2169–2183. https://doi.org/10.5194/amt-7-2169-2014.

Caputo, A., Di Cristofato, E., Gonella, B., Taurino, E., 2022. Il metano nell'Inventario nazionale delle emissioni di gas serra. In: L'Italia e il Global Methane Pledge. Istituto Superiore Protezione E Ricerca Ambientale. URL. https://www.isprambiente.gov.it/it/pubblicazioni/rapporti/il-metano-nell2019inventario-nazionale-delle-emissioni-di-gas-serra-l2019italia-e-il-global-methane-pledge. (Accessed 12 December 2022).

Cheewaphongphan, P., Chatani, S., Saigusa, N., 2019. Exploring gaps between bottom-up and top-down emission estimates based on uncertainties in multiple emission inventories: a case study on CH4 emissions in China. Sustainability 11, 2054. https://doi.org/10.3390/su11072054.

Chen, Z., Griffis, T.J., Baker, J.M., Millet, D.B., Wood, J.D., Dlugokencky, E.J., Andrews, A.E., Sweeney, C., Hu, C., Kolka, R.K., 2018. Source partitioning of methane emissions and its seasonality in the U.S. Midwest. J. Geophys. Res. Biogeosciences 123, 646–659. https://doi.org/10.1002/2017JG004356.

Couret, C., 2022. Atmospheric CO at Zugspitze-Schneefernerhaus by German Environment Agency , Dataset Published as CO_ZSF_ surface-insitu_UBAG_data1 at WDCGG, Ver. 2022-05-03-0856 (Reference Date: 2023/04/29).

Crippa, M., Janssens-Maenhout, G., Dentener, F., Guizzardi, D., Sindelarova, K., Muntean, M., Van Dingenen, R., Granier, C., 2016. Forty years of improvements in European air quality: regional policy-industry interactions with global impacts. Atmos. Chem. Phys. 16, 3825–3841. https://doi.org/10.5194/acp-16-3825-2016.

Crippa, M., Guizzardi, D., Muntean, M., Schaaf, E., Dentener, F., van Aardenne, J.A., Monni, S., Doering, U., Olivier, J.G.J., Pagliari, V., Janssens-Maenhout, G., 2018. Gridded emissions of air pollutants for the period 1970–2012 within EDGAR v4.3.2. Earth Syst. Sci. Data 10, 1987–2013. https://doi.org/10.5194/essd-10-1987-2018.

Crippa, M., Solazzo, E., Huang, G., Guizzardi, D., Koffi, E., Muntean, M., Schieberle, C., Friedrich, R., Janssens-Maenhout, G., 2019. High resolution temporal profiles in the emissions database for global atmospheric research (EDGAR). Sci. Data 7, 121. https://doi:10.1038/s41597-020-0462-2.

Crippa, M., Guizzardi, D., Muntean, M., Schaaf, E., Lo Vullo, E., Solazzo, E., Monforti-Ferrario, F., Olivier, J., Vignati, E., 2021. EDGAR v6.0 Greenhouse Gas Emissions. European Commission, Joint Research Centre (JRC). PID. http://data.europa.eu/89h/97a67d67-c62e-4826-b873-9d972c4f670b.

Crippa, M., Guizzardi, D., Muntean, M., Schaaf, E., Monforti-Ferrario, F., Banja, M., Pagani, F., Solazzo, E., 2022. EDGAR v6.1 Global Air Pollutant Emissions. European Commission, Joint Research Centre (JRC). PID.

Cristofanelli, P., Arduini, J., Calzolari, F., Giostra, U., Bonasoni, P., Maione, M., 2020. First evidences of methyl chloride (CH_3Cl) transport from the northern Italy boundary layer during summer 2017. Atmosphere 11, 238. https://doi.org/10.3390/atmos11030238.

Cristofanelli, P., Arduini, J., Maione, M., 2021a. Atmospheric CO at Monte Cimone by National Research Council, Institute of Atmospheric Sciences and Climate. dataset published as CO_CMN_surface-insitu_ISAC_data1 at WDCGG, ver.2021-06-21-1409, Reference date: 2022/06/27.

Cristofanelli, P., Fierli, F., Marinoni, A., Calzolari, F., Duchi, R., Burkhart, J., Stohl, A., Maione, M., Arduini, J., Bonasoni, P., 2013. Influence of biomass burning and anthropogenic emissions on ozone, carbon monoxide and black carbon at the Mt. Cimone GAW-WMO global station (Italy, 2165 m a.s.l.). Atmos. Chem. Phys. 13, 15–30. https://doi.org/10.5194/acp-13-15-2013.

Cristofanelli, P., Gutiérrez, I., Adame, J.A., Bonasoni, P., Busetto, M., Calzolari, F., Putero, D., Roccato, F., 2021b. Interannual and seasonal variability of NOx observed at the Mt. Cimone GAW/WMO global station (2165 m a.s.l., Italy). Atmos. Environ. 249, 118245 https://doi.org/10.1016/j.atmosenv.2021.118245.

Cristofanelli, P., Trisolino, P., 2022a. ICOS ATC CH4 Release, Monte Cimone (8.0 M), 2018-05-03–2022-02-28. ICOS RI. https://hdl.handle.net/11676/NrfOOu7HCEcxG1VHnjUCmZIW. (Accessed 11 November 2022).

Cristofanelli, P., Trisolino, P., 2022b. ICOS ATC CO Release, Monte Cimone (8.0 M), 2018-05-03–2022-02-28. ICOS RI. https://hdl.handle.net/11676/mj51O1-n-AI3ip3WVmRe4apK. (Accessed 11 November 2022).

Deng, Z., Ciais, P., Tzompa-Sosa, Z.A., Saunois, M., Qiu, C., Tan, C., Sun, T., Ke, P., Cui, Y., Tanaka, K., Lin, X., Thompson, R.L., Tian, H., Yao, Y., Huang, Y., Lauerwald, R., Jain, A.K., Xu, X., Bastos, A., Sitch, S., Palmer, P.I., Lauvaux, T., d'Aspremont, A., Giron, C., Benoit, A., Poulter, B., Chang, J., Petrescu, A.M.R., Davis, S.J., Liu, Z., Grassi, G., Albergel, C., Tubiello, F.N., Perugini, L., Peters, W., Chevallier, F., 2022. Comparing national greenhouse gas budgets reported in

UNFCCC inventories against atmospheric inversions. Earth Syst. Sci. Data 14, 1639–1675. https://doi.org/10.5194/essd-14-1639-2022.
D'Onofrio, C., 2021. ICOS Carbon Portal. ICOS Carbon-Portal python library. https://github.com/ICOS-Carbon-Portal/pylib. URL.
Drewnick, F., Böttger, T., von der Weiden-Reinmüller, S.-L., Zorn, S.R., Klimach, T., Schneider, J., Borrmann, S., 2012. Design of a mobile aerosol research laboratory and data processing tools for effective stationary and mobile field measurements. Atmos. Meas. Tech. 5, 1443–1457. https://doi.org/10.5194/amt-5-1443-2012.
Eggleston, H.S., Buendia, L., Miwa, K., Ngara, T., Tanabe, K., 2006. 2006 IPCC guidelines for national greenhouse gas inventories. URL. https://www.ipcc-nggip.iges.or.jp/public/2006gl/.
El Yazidi, A., Ramonet, M., Ciais, P., Broquet, G., Pison, I., Abbaris, A., Brunner, D., Conil, S., Delmotte, M., Gheusi, F., Guerin, F., Hazan, L., Kachroudi, N., Kouvarakis, G., Mihalopoulos, N., Rivier, L., Serça, D., 2018. Identification of spikes associated with local sources in continuous time series of atmospheric CO, CO_2 and CH_4. Atmos. Meas. Tech. 11, 1599–1614. https://doi.org/10.5194/amt-11-1599-2018.
Flerlage, H., Velders, G.J.M., de Boer, J., 2021. A review of bottom-up and top-down emission estimates of hydrofluorocarbons (HFCs) in different parts of the world. Chemosphere 283, 131208. https://doi.org/10.1016/j.chemosphere.2021.131208.
Giostra, U., Furlani, F., Arduini, J., Cava, D., Manning, A.J., O'Doherty, S.J., Reimann, S., Maione, M., 2011. The determination of a "regional" atmospheric background mixing ratio for anthropogenic greenhouse gases: a comparison of two independent methods. Atmos. Environ. 45, 7396–7405. https://doi.org/10.1016/j.atmosenv.2011.06.076.
Hazan, L., Tarniewicz, J., Ramonet, M., Laurent, O., Abbaris, A., 2016. Automatic processing of atmospheric CO_2 and CH_4 mole fractions at the ICOS atmosphere thematic Centre. Atmos. Meas. Tech. 9, 4719–4736. https://doi.org/10.5194/amt-9-4719-2016.
Heiskanen, J., Brümmer, C., Buchmann, N., Calfapietra, C., Chen, H., Gielen, B., Gkritzalis, T., Hammer, S., Hartman, S., Herbst, M., Janssens, I.A., Jordan, A., Juurola, E., Karstens, U., Kasurinen, V., Kruijt, B., Lankreijer, H., Levin, I., Linderson, M.-L., Loustau, D., Merbold, L., Myhre, C.L., Papale, D., Pavelka, M., Pilegaard, K., Ramonet, M., Rebmann, C., Rinne, J., Rivier, L., Saltikoff, E., Sanders, R., Steinbacher, M., Steinhoff, T., Watson, A., Vermeulen, A.T., Vesala, T., Vítková, G., Kutsch, W., 2022. The integrated carbon observation system in Europe. Bull. Am. Meteorol. Soc. 103, E855–E872. https://doi.org/10.1175/BAMS-D-19-0364.1.
ICOS, R.I., Bergamaschi, P., Colomb, A., De Mazière, M., Emmenegger, L., Kubistin, D., Lehner, I., Lehtinen, K., Leuenberger, M., Lund Myhre, C., Marek, M., Platt, S.M., Plaß-Dülmer, C., Ramonet, M., Schmidt, M., Apadula, F., Arnold, S., Chen, H., Conil, S., Couret, C., Cristofanelli, P., Forster, G., Hatakka, J., Heliasz, M., Hermansen, O., Hoheisel, A., Kneuer, T., Laurila, T., Leskinen, A., Levula, J., Lindauer, M., Lopez, M., Mammarella, I., Manca, G., Meinhardt, F., Müller-Williams, J., Ottosson-Löfvenius, M., Piacentino, S., Pitt, J., Scheeren, B., Schumacher, M., Sha, M.K., Smith, P., Steinbacher, M., Sørensen, L.L., Vítková, G., Yver-Kwok, C., di Sarra, A., Conen, F., Kazan, V., Roulet, Y.-A., Biermann, T., Delmotte, M., Heltai, D., Komínková, K., Laurent, O., Lunder, C., Marklund, P., Pichon, J.-M., Trisolino, P., ICOS Atmosphere Thematic Centre, ICOS ERIC - Carbon Portal, ICOS Flask And Calibration Laboratory (FCL), ICOS Flask And Calibration Laboratory (FCL), ICOS Central Radiocarbon Laboratory (CRL), 2022. ICOS Atmosphere Release 2022-1 of Level 2 Greenhouse Gas Mole Fractions of CO_2, CH_4, N_2O, CO, Meteorology and $^{14}CO_2$. https://doi.org/10.18160/KCYX-HA35.
Istituto Superiore per la Protezione e la Ricerca Ambientale, 2022. La disaggregazione a livello provinciale dell'inventario nazionale delle emissioni. Report of Ist. Super. Prot. E Ric. Ambient. Volume 369/2022, pag 185. URL https://www.isprambiente.gov.it/it/pubblicazioni/rapporti/la-disaggregazione-a-livello-provinciale-dell2019inventario-nazionale-delle-emissioni. (Accessed 17 November 2022).
Italian Air Force Mountain Centre (IAFMS), 2022. Atmospheric CH4 at Monte Cimone by Italian Air Force Mountain Centre (IAFMS) , Dataset Published as CH4 _ CMN _ Surface - Insitu _ IAFMS _ Data1 at WDCGG, ver.2022-05-04-1246. Reference date: 2022/06/27.
Japan Meteorological Agency and World Meteorological Organization, 2022. WMO WDCGG Data Summary -WDCGG No. 46. GAW DATA Volume IV-Greenhouse and Related Gases. https://gaw.kishou.go.jp/static/publications/summary/sum46/sum46.pdf.
Kuwayama, T., Charrier-Klobas, J.G., Chen, Y., Vizenor, N.M., Blake, D.R., Pongetti, T., Conley, S.A., Sander, S.P., Croes, B., Herner, J.D., 2019. Source apportionment of ambient methane enhancements in Los Angeles, California, to evaluate emission inventory estimates. Environ. Sci. Technol. 53, 2961–2970. https://doi.org/10.1021/acs.est.8b02307.
Le Quéré, C., Jackson, R.B., Jones, M.W., Smith, A.J.P., Abernethy, S., Andrew, R.M., De-Gol, A.J., Willis, D.R., Shan, Y., Canadell, J.G., Friedlingstein, P., Creutzig, F., Peters, G.P., 2020. Temporary reduction in daily global CO_2 emissions during the COVID-19 forced confinement. Nat. Clim. Change 10, 647–653. https://doi.org/10.1038/s41558-020-0797-x.
Lin, J.C., Gerbig, C., Wofsy, S.C., Andrews, A.E., Daube, B.C., Davis, K.J., Grainger, C.A., 2003. A near-field tool for simulating the upstream influence of atmospheric observations: the Stochastic Time-Inverted Lagrangian Transport (STILT) model. J. Geophys. Res. Atmospheres 108. https://doi.org/10.1029/2002JD003161.
Meijidea, A., Grueningb, C., Godedb, I., Seufertb, G., Cescatti, A., 2017. Water management reduces greenhouse gas emissions in a Mediterranean rice paddy field. Agric. Ecosyst. Environ. 238, 168–178. https://doi.org/10.1016/j.agee.2016.08.017.
Nisbet, E., Weiss, R., 2010. Top-down versus bottom-up. Science 328, 1241–1243. https://doi.org/10.1126/science.1189936.
Pezzagno, M., Richiedei, A., Tira, M., 2020. Spatial planning policy for sustainability: analysis connecting land use and GHG emission in rural areas. Sustainability 12, 947. https://doi.org/10.3390/su12030947.
Plant, G., Kort, E.A., Murray, L.T., Maasakkers, J.D., Aben, I., 2022. Evaluating urban methane emissions from space using TROPOMI methane and carbon monoxide observations. Remote Sens. Environ. 268, 112756 https://doi.org/10.1016/j.rse.2021.112756.
Ren, X., Salmon, O.E., Hansford, J.R., Ahn, D., Hall, D., Benish, S.E., Stratton, P.R., He, H., Sahu, S., Grimes, C., Heimburger, A.M.F., Martin, C.R., Cohen, M.D., Stunder, B., Salawitch, R.J., Ehrman, S.H., Shepson, P.B., Dickerson, R.R., 2018. Methane emissions from the baltimore-Washington area based on airborne observations: comparison to emissions inventories. J. Geophys. Res. Atmospheres 123, 8869–8882. https://doi.org/10.1029/2018JD028851.
Romano, D., Arcarese, C., Bernetti, A., Caputo, A., Cordella, M., De Lauretis, R., Di Cristoforo, E., Gagna, A., Gonella, B., Moricci, F., Pellis, G., Taurino, E., Vitullo, Marina, 2022. Italian greenhouse gas inventory. ISPRA - Ist. Super. Prot. E Ric. Ambient. Annual Report for submission under the UN Framework Convention on Climate Change and the Kyoto Protocol 623.
Saunois, M., Stavert, A.R., Poulter, B., Bousquet, P., Canadell, J.G., Jackson, R.B., Raymond, P.A., Dlugokencky, E.J., Houweling, S., Patra, P.K., Ciais, P., Arora, V.K., Bastviken, D., Bergamaschi, P., Blake, D.R., Brailsford, G., Bruhwiler, L., Carlson, K.M., Carrol, M., Castaldi, S., Chandra, N., Crevoisier, C., Crill, P.M., Covey, K., Curry, C.L., Etiope, G., Frankenberg, C., Gedney, N., Hegglin, M.I., Höglund-Isaksson, L., Hugelius, G., Ishizawa, M., Ito, A., Janssens-Maenhout, G., Jensen, K.M., Joos, F., Kleinen, T., Krummel, P.B., Langenfelds, R.L., Laruelle, G.G., Liu, L., Machida, T., Maksyutov, S., McDonald, K.C., McNorton, J., Miller, P.A., Melton, J.R., Morino, I., Müller, J., Murguia-Flores, F., Naik, V., Niwa, Y., Noce, S., O'Doherty, S., Parker, R.J., Peng, C., Peng, S., Peters, G.P., Prigent, C., Prinn, R., Ramonet, M., Regnier, P., Riley, W.J., Rosentreter, J.A., Segers, A., Simpson, I.J., Shi, H., Smith, S.J., Steele, L.P., Thornton, B.F., Tian, H., Tohjima, Y., Tubiello, F.N., Tsuruta, A., Viovy, N., Voulgarakis, A., Weber, T.S., van Weele, M., van der Werf, G.R., Weiss, R.F., Worthy, D., Wunch, D., Yin, Y., Yoshida, Y., Zhang, W., Zhang, Z., Zhao, Y., Zheng, B., Zhu, Qing, Zhu, Qiuan, Zhuang, Q., 2020. The global methane budget 2000–2017. Earth Syst. Sci. Data 12, 1561–1623. https://doi.org/10.5194/essd-12-1561-2020.
Seitz, T., 2022. Atmospheric CO at Payerne by Swiss Federal Laboratories for Materials Science and Technology. dataset published as CO_PAY_ surface-insitu_Empa_data1 at WDCGG, ver. 2022-06-30-1312 (Reference date: 2023/04/29).
Seitz, T., Steinbacher, M., 2022. Atmospheric CO at Jungfraujoch by Swiss Federal Laboratories for Materials Science and Technology. dataset published as CO_JFJ_surface-insitu_Empa_data1 at WDCGG, ver. 2022-07-06-1450. https://doi.org/10.50849/WDCGG_0023-6036-3001-01-01-9999 (Reference date: 2023/04/29.
Silva, S.J., Arellano, A.F., Worden, H.M., 2013. Toward anthropogenic combustion emission constraints from space-based analysis of urban CO_2/CO sensitivity. Geophys. Res. Lett. 40, 4971–4976. https://doi.org/10.1002/grl.50954.
Solazzo, E., Crippa, M., Guizzardi, D., Muntean, M., Choulga, M., Janssens-Maenhout, G., 2021. Uncertainties in the emissions database for global atmospheric research (EDGAR) emission inventory of greenhouse gases. Atmos. Chem. Phys. 21, 5655–5683. https://doi.org/10.5194/acp-21-5655-2021.
Spangl, W., Buxbaum, I., 2022. Atmospheric CO at SONNBLICK Observatory by Federal Environment Agency Austria , Dataset Published as CO_SNB_ surface-insitu_UBAA_data1 at WDCGG. ver. 2022-07-21-0648 (Reference date: 2023/04/29).
Steinbacher, M., 2022. Atmospheric CH_4 at Jungfraujoch by Swiss Federal Laboratories for Materials Science and Technology. dataset published as CH4_JFJ_surface-insitu_Empa_data1 at WDCGG, ver.2022-07-06-1450, Reference date: 2022/12/10.
Szopa, S., Naik, V., Adhikary, B., Artaxo, P., Berntsen, T., Collins, W.D., Fuzzi, S., Gallardo, L., Kiendler-Scharr, A., Klimont, Z., Liao, H., Unger, N., Zanis, P., 2021. Short-lived climate forcers. Clim. Change 2021 Phys. Sci. Basis Contrib. Work. Group Sixth Assess. Rep. Intergov. Panel Clim. Change. https://doi.org/10.1017/9781009157896.008.
Thoning, K.W., Tans, P.P., Komhyr, W.D., 1989. Atmospheric carbon dioxide at mauna loa observatory: 2. Analysis of the NOAA GMCC data, 1974–1985. J. Geophys. Res. Atmospheres 94, 8549–8565. https://doi.org/10.1029/JD094iD06p08549.
Trisolino, P., di Sarra, A., Sferlazzo, D., Piacentino, S., Monteleone, F., Di Iorio, T., Apadula, F., Heltai, D., Lanza, A., Vocino, A., Caracciolo di Torchiarolo, L., Bonasoni, P., Calzolari, F., Busetto, M., Cristofanelli, P., 2021. Application of a common methodology to select in situ CO_2 observations representative of the atmospheric background to an Italian collaborative network. Atmosphere 12, 246. https://doi.org/10.3390/atmos12020246.
World Meteorological Organization, 2022. WMO Greenhouse Gas Bulletin, No. 18, 26 October 2022. ISSN 2078-0796. https://library.wmo.int/doc_num.php?explnum_id=11352.
Worthy, D.E.J., Chan, E., Ishizawa, M., Chan, D., Poss, C., Dlugokencky, E.J., Maksyutov, S., Levin, I., 2009. Decreasing anthropogenic methane emissions in Europe and Siberia inferred from continuous carbon dioxide and methane observations at Alert, Canada. J. Geophys. Res. Atmos. 114 https://doi.org/10.1029/2008JD011239.
Yver-Kwok, C., Philippon, C., Bergamaschi, P., Biermann, T., Calzolari, F., Chen, H., Conil, S., Cristofanelli, P., Delmotte, M., Hatakka, J., Heliasz, M., Hermansen, O., Komínková, K., Kubistin, D., Kumps, N., Laurent, O., Laurila, T., Lehner, I., Levula, J., Lindauer, M., Lopez, M., Mammarella, I., Manca, G., Marklund, P., Metzger, J.-M., Mölder, M., Platt, S.M., Ramonet, M., Rivier, L., Scheeren, B., Sha, M.K., Smith, P., Steinbacher, M., Vítková, G., Wyss, S., 2021. Evaluation and optimization of ICOS atmosphere station data as part of the labeling process. Atmos. Meas. Tech. 14, 89–116. https://doi.org/10.5194/amt-14-89-2021.